Dynamic structure factor of a one-dimensional Peierls system

Tutiš, Eduard; Barišić, Slaven

Dynamic structure factor of a one-dimensional Peierls system

E. Tutiš
Institute of Physics of the University, POB 304, Zagreb, Croatia, Yugoslavia

S. Barišić
Department of Physics, Faculty of Sciences, POB 162, Zagreb, Croatia, Yugoslavia
(Received 16 July 1990; revised manuscript received 2 October 1990)

The Newtonian dynamics of a one-dimensional system with a complex order parameter and an anharmonic potential energy of the Landau type is examined in a wide temperature range using numerical Monte Carlo–molecular dynamics simulations. Results are discussed with an emphasis on the incommensurate Peierls systems. Dispersive-mode behavior found previously in the quartic region near $T_{\rm MF}$ can be followed to lower temperatures where the frequency of the phonon mode decreases and the damping increases. Below $0.4T_{\rm MF}$ the dynamic structure factor is characterized by the overdamped mode down to $0.3T_{\rm MF}$, when the separation between the phase and the amplitude mode becomes effective. The relation between the different regimes in $S(k,\omega)$ and the pseudogap in the electronic spectrum is also briefly discussed.

INTRODUCTION

The lattice dynamics of several quasi-one-dimensional chain compounds has been studied carefully in a wide temperature range during the last 15 years.[1,2] Particular attention has been paid to the dynamics of phonons with wave vectors close to the wave vector of the Peierls transition. These measurements gave the dynamic structure factor with an underdamped phonon mode at high temperatures which first transforms to the overdamped structure as the temperature is lowered and then to the phase and amplitude modes at low temperatures. In addition, the sharp central ($\omega=0$) peak is observed in the vicinity of the temperature T_p, where the three-dimensional phase transition occurs.

The interpretation of these features requires a clear separation between the effects of the strong one-dimensional correlations and the effects of the interchain coupling, which finally leads to the Peierls transition at a finite temperature. In this paper we address the question of the dynamics of a strictly one-dimensional system and argue that all described features except for the central peak at T_p may be understood within this framework. The various temperature regimes are determined. It appears that the conventional picture in which the amplitude-phase separation is usually assumed to hold immediately below the one-dimensional mean-field transition temperature $T_{\rm MF}$ is incorrect. Instead, we obtain a well-defined underdamped phonon around $T_{\rm MF}$ and the amplitude-phase separation starts only below $0.3T_{\rm MF}$ preceded by a temperature region between $0.4T_{\rm MF}$ and $0.3T_{\rm MF}$ in which the Peierls phonon is overdamped. Our results are relevant to experiments on chain compounds that are carried out in the one-dimensional region above the temperature of the dimensional crossover T_x. However, some qualitative features remain unchanged, even when the interchain coupling is included, as can be seen from experiments, except for the occurrence of the central peak near T_p, which seems to superimpose to the one-dimensional (1D) behavior.

MODEL

The model of the one-dimensional system considered here is given by the Lagrangian

$$L=\int dx\,[m|\partial_t\psi|^2-c|\partial_x\psi|^2-a|\psi|^2-(b/4)|\psi|^4]\ . \tag{1}$$

In the Peierls system the complex field $\psi(x)=[\psi_1(x)+i\psi_2(x)]/\sqrt{2}$ describes the deformations of the lattice with wave vectors near $2k_F$ (in what follows we measure the wave vector in the Peierls systems relative to $2k_F$). The coefficients of the Lagrangian for the Peierls system are obtained[3] from the high-temperature Landau expansion of the electronic free energy with respect to deformation. The result is

$$\begin{aligned} a&=a'\ln(T/T_{\rm MF})\\ &\approx a'(T/T_{\rm MF}-1)\ \text{ near } T_{\rm MF}\ ,\\ a'&=\lambda m\omega_0^2\ ,\\ b&=[7\zeta(3)/8\pi]v_F(a'/T)^2\ ,\\ c&=2a'v_F^2/(2\pi T)^2\ . \end{aligned} \tag{2}$$

Here $\lambda<1$ denotes a dimensionless electron-phonon coupling constant, m is the mass of the system per unit cell, and ω_0 is the bare phonon frequency. Below $T_{\rm MF}$ the values of all coefficients are fixed to their values at $T_{\rm MF}$ except for the coefficient a in which the dependence of the form $(T/T_{\rm MF}-1)$ is retained. This procedure gives a correct description of phonons for $T\ll T_{\rm MF}$ apart from some numerical factors of the order of unity that emerge in the low-temperature approach.[4] A similar Lagrangian applies in the case when the electrons corre-

lated by Coulomb interactions ($g > \lambda$) follow the lattice adiabatically.[5] Note that the Lagrangian (1) describes a system with inertial dynamics—the damping effects which come, for example, from nonadiabatic corrections of the electronic response to the phonon field or from impurities are not taken into account. It turns out, in fact, that the damping effects which come from the nonlinearities in the Lagrangian (1) are dominant in $S(k,\omega)$ over other sources of damping in the 1D Peierls system.

We are going to consider the dynamics of the system in the temperature range where it behaves classically and calculate its dynamical structure factor $S(k,\omega)$ defined as

$$S(k,\omega)=\int dt\,dx\,\langle\psi_1(x,t)\psi_1(,0)\rangle\exp(-ikx+i\omega t)$$
$$=\int dt\,dx\,\langle\psi_2(x,t)\psi_2(0,0)\rangle\exp(-ikx+i\omega t)\ . \tag{3}$$

GENERAL PROPERTIES OF $S(k,\omega)$

It is convenient to express the results for the dynamic structure factor (3) in terms of reduced variables. The dimensional analysis shows that only one dimensionless parameter can be obtained from the coefficients of the Lagrangian (1) and the temperature T. It is

$$\vartheta=(bT/|a|c)(c/|a|)^{1/2}\ . \tag{4}$$

This parameter plays the role of a reduced temperature. For the Peierls system [see Eqs. (2)], it is a function of $T/T_{\rm MF}$ only:

$$\vartheta=\tfrac{3}{2}(T/T_{\rm MF})(1-T/T_{\rm MF})^{-3/2}\ . \tag{5}$$

The dynamic structure factor $S(k,\omega)$ may be written using a dimensionless function s as

$$S(k,\omega)=[(mc)^{1/2}/b\,]s(\vartheta,k/K,\omega/\Omega)\ , \tag{6}$$

where Ω and K are appropriate combinations of m, a, b c, and T with dimensions of the frequency and wave vector, respectively. Note that the choice of Ω and K is not unique since an extra factor which is a function of ϑ does not change their dimension. In fact, the choice of Ω and K fixes the definition of s. Note also that, although Ω and K may be temperature dependent, the form (profile) of $S(k,\omega)$ is determined by ϑ only (or $T/T_{\rm MF}$ in the Peierls case) since K and Ω are only the affinity factors of this form.

Let us mention some possible choices for Ω and K. Two of them are

$$\Omega_b=m^{-1/2}(bT/c^{1/2})^{1/3}\ ,$$
$$K_b=c^{-1/2}(bT/c^{1/2})^{1/3}\ , \tag{7}$$

and

$$\Omega_a=(|a|/m)^{1/2},\quad K_a=(|a|/c)^{1/2}\ . \tag{8}$$

The first one is appropriate for the Peierls system for $T/T_{\rm MF}\sim 1$, but not for $T/T_{\rm MF}\ll 1$ since $\Omega_b, K_b\to 0$ as $T/T_{\rm MF}\to 0$. The reverse is true for the second choice. Therefore, in order to present $S(k,\omega)$ in both temperature regions, it seems convenient to make a choice for Ω (and K) which is neither Ω_a (K_a) nor Ω_b (K_b), but the sum of them:

$$\Omega\equiv\Omega_a+\Omega_b,\quad K\equiv K_a+K_b\ . \tag{9}$$

The dependence of the affinity factors Ω, K, and $(mc)^{1/2}/b$ on the temperature in the Peierls case are given in Table I.

TABLE I. Temperature dependence of scales for the Peierls system for $t\equiv T/T_{\rm MF}\le 1$.

$\vartheta=0.375t/(1-t)^{3/2}$
$\Omega_b=1.14\lambda^{1/2}\omega_0 t^{1/3}$
$\Omega_a=\lambda^{1/2}\omega_0(1-t)^{1/2}$
$K_b=5.07(T_{\rm MF}/v_F)t^{1/3}$
$K_a=4.44(T_{\rm MF}/v_F)(1-t)^{1/2}$
$u=0.23\lambda^{1/2}\omega_0(v_F/T_{\rm MF})$
$(mc)^{1/2}/b=0.672T_{\rm MF}/(\lambda^{3/2}m\omega_0^3)$

NUMERICAL METHOD

The calculation of the universal function $s(\vartheta,\kappa,\nu)$ is done by simulating the system numerically. We use for that purpose the discrete counterpart of the system described by the Lagrangian (1):

$$L=\sum_n[m|\partial_t\psi_n|^2-c|\psi_{n+1}-\psi_n|^2$$
$$-a|\psi_n|^2-(b/4)|\psi_n|^4]\ , \tag{10}$$

where the distance between succeeding nodes is taken as unity. It should be further noted that the numerical values of the parameters of the Lagrangian, m, a, b, c, and the temperature T, that one uses in the simulation (denoting them by m_s, a_s, b_s, c_s, and T_s, respectively) need not be those found in real physical systems. Only the values of the reduced, dimensionless variables ϑ, κ, and ν are important. Moreover, even m_s, a_s, b_s, c_s, and T_s may be taken as dimensionless. A typical set of values that we use is $m_s=2$, $a_s=-2$, $b_s=8$, $c_s=2$, and $T_s=0.4$. Different values leading to the same ϑ, κ, and ν are used to check the scaling property of $S(k,\omega)$ given by Eqs. (6)–(9). Various sets of parameters are also used to test the effects of discreteness and the effect of the finite size of the system. These tests finally allow us to perform the simulations on a relatively small system consisting of 128 nodes (particles) with periodic boundary conditions.

The numerical simulation is a combination of Monte Carlo (MC) and molecular dynamics (MD) methods. The Monte Carlo method is used to generate the initial configurations in the phase space for the MD runs. For each set of parameters, we perform 20 MC runs. From each of these runs, 20 configurations are extracted. The MD evolution is performed on these 400 configurations using the algorithm proposed by Beeman.[6] The typical time step $h_s=0.2$ is short enough to ensure energy conservation during runs to a few parts per thousand. MD runs are relatively short (1280 steps), but long enough to ensure good resolution in frequency. The structure factor for each wave vector is found as an average over 400 Fourier transforms.

Returning to the Monte Carlo part of the calculation, one first recognizes that the Maxwell distribution for velocities of particles may be directly generated by the usual means of producing normal distributions. The problem is actually to generate the Boltzmann distribution for the particle positions. Because of the quartic term in the potential energy, the direct procedure is not possible in this case. Instead, we use the well-known metropolis algorithm to generate a large number of configurations. However, even then, the starting configuration for the metropolis sequence should not be chosen entirely at random since that would require a very long "thermalization" part of the MC run. A possible way to choose a suitable starting configuration is to find some approximate scheme of solving for the distribution (i.e., producing its representative members). One way to do that is to consider the independent nodes ($c=0$) first and solve the distribution for the moduli $|\psi_n|$ of the vectors describing the particle positions. The angles $(\chi_{n+1}-\chi_n)$ between succeeding vectors are produced as the second step using the modified distribution in which the term $c|\psi_n-\psi_{n+1}|^2$ is replaced by $c|\psi_n||\psi_{n+1}|(\chi_n-\chi_{n+1})^2$. Both steps may be performed using the normal distribution generators. The thermalization part of the MC run consists of 800 sweeps along the chain in which the metropolis procedure is repeated on each particle. The configurations used for the molecular-dynamics calculations are then taken after every 300 sweeps in order to reduce their mutual correlation.

Let us mention a few ways in which the errors that may arise in this approach may be estimated and controlled.

(i) The effect of discreteness may be considered as unimportant if the correlation length is much larger than unity (lattice constant). We evaluate the static structure factor using only the MC method as well as using the configurations obtained during the MD runs. The results are consistent, indicating that the error is always less than 1% for the integral $\int dk\, S(k)$. The correlation length is found to be between 5 and 15 lattice units. Its temperature dependence is checked against transfer-matrix calculations,[7] showing a very good agreement.

(ii) In the MD evolution we control not only the conservation of the overall energy, but also the conservation of the angular momentum with respect to the axis perpendicular to the (ψ_1,ψ_2) plane. This also indicates an error of the order of one part per thousand (measured relative to the $|\psi|_{\rm rms}|\partial_t\psi|_{\rm rms}$).

(iii) The symmetry of the system with respect to exchange of ψ_1 and ψ_2 [see Eq. (3)] may be used to estimate the error in $s(\vartheta,\kappa,\nu)$. The relative error for the integral of this quantity over ω is of the order of 1%.

(iv) The quality of the initial configuration given by MC runs may be tested by comparing the ratio of the total potential and kinetic energies before and after the MD evolution. The difference is not significant. Similar tests show that the temperature of the system measured in the molecular dynamics as a mean kinetic energy and the temperature that enters as a parameter in the Monte Carlo procedure do not differ very much. We find $T_{\rm MC}=\langle T_{\rm MD}\rangle+\Delta T_{\rm MD}$ with $\Delta T_{\rm MD}/T_{\rm MC}\sim 0.02$. In general, the static averages may be done using the MC method only and compared with the results of the MC-MD method we just described. We compared the potential energy and static correlation functions, which again indicates an error of the order of 1%.

Finally, we would like to say that this combination of MC and MD methods was not, to our knowledge, used very much in the literature (a similar scheme was proposed in Ref. 8). However, the method itself has several advantages. The most important are the following.

(a) The method is much better than the pure molecular dynamics for systems in which some kind of decoupling between different subsystems (or degrees of freedom) exists. It is generally very difficult to realize whether or not the decoupling exists to some extent. In our system we know that the system becomes quasiharmonic much above (phonons) and much below (amplitudons and phasons) the mean-field transition temperature $T_{\rm MF}$. In these regimes the molecular-dynamics method (in which the contact with the external thermal bath is not explicitly included) would require a very long run to sample the entire phase space (for our system the movement in the k space is very slow). In the MC-MD method the MD runs start with many different and representative initial configurations, and this problem does not appear.

(b) The temperature of the system for the molecular-dynamics calculation may be easily chosen from the beginning. There is no need for various procedures of "heating" and "cooling." The thermalization part of the MD run is not needed either.

RESULTS

The function $s(\vartheta,\kappa,\nu)$ for $\kappa=0$ is shown in Figs. 1 and 2 for different values of the parameter ϑ [or $T/T_{\rm MF}$ via Eq. (5)]. For special values of ϑ ($\vartheta=0.20$, $\vartheta=2.0$, $\vartheta=\infty$), the dependence of $s(\vartheta,\kappa,\omega)$ on the wave vector κ is shown in Figs. 3(a), 4, and 5. Since $S(k,\omega)$ is an even function of ω, only the $\omega\geq 0$ part is shown.

We start our discussion with high temperatures. The frequency of the $k=0$ phonon diminishes and the damping increases as the temperature is lowered toward $T_{\rm MF}$. However, the frequency of the $k=0$ phonon is finite at $T=T_{\rm MF}$, as can be seen from Fig. 5, although the quadratic a term in the Lagragian (1) vanishes. Note that $a=0$ corresponds to the complete softening in the conventional picture of the Peierls-Kohn phonon where the quartic b term is neglected. The dispersion of the phonon branch starts at $\omega_Q=0.71\Omega_b$, while the dependence on the wave vector follows from the Lorentz invariance of the Lagrangian with the characteristic velocity

$$u\equiv(c/m)^{1/2}\ . \tag{11}$$

For the Peierls case the ratio of the frequency ω_Q and the frequency $\omega_Q=\lambda^{1/2}\omega_0$ of the amplitude mode obtained from the $T=0$ approach[4,9] is a pure number 0.62. The ratio found in blue bronze ($T_{\rm MF}=320$ K; see Ref. 10) is 0.71, not very far from our result. The difference is probably due to the interchain coupling effects, which, although small, are not entirely negligible. The damping of the phonon may be also read from Fig. 5. At $k=0$ the

damping constant (half width at half maximum) is 10% of the frequency. The damping measured[10] in blue bronze is of the same order of magnitude. Considering the finite frequency at $k=0$, it may be interesting to compare ω_Q with the result of the Hartree or Hartree-Fock approximation for the nonlinear term in the Lagrangian (1). It turns out that ω_Q is between ω_H and ω_{HF}, $\omega_Q=1.13\omega_H=0.89\omega_{\mathrm{HF}}$. However, the artifact of these approximations when applied to local interactions is the absence of damping, and this becomes a qualitative problem when the temperature is lowered further.

What happens on lowering the temperature is shown in Fig. 2. The frequency of the $k=0$ phonon diminishes, the damping increases, and for $T/T_{\mathrm{MF}}<0.4$ ($\vartheta=1.40$)

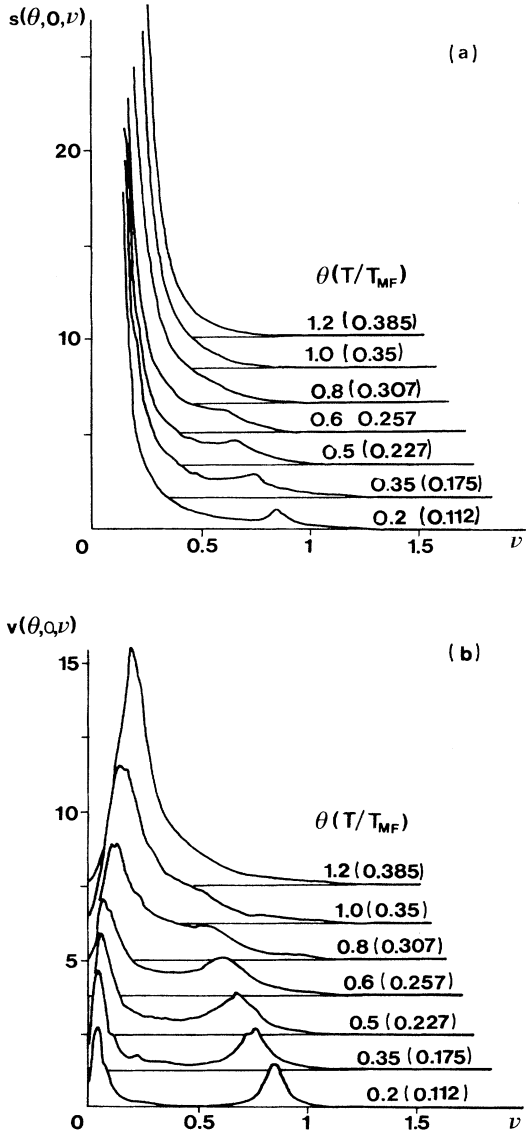

FIG. 1. (a) Dynamic structure factor as a function of frequency for different temperatures ($T/T_{\mathrm{MF}}<0.4$). Reduced variables are used as explained in the text. (b) Velocity-velocity correlation function.

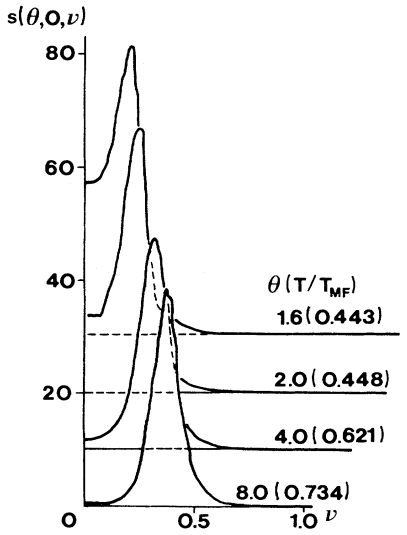

FIG. 2. Same as Fig. 1(a), but for $T/T_{\mathrm{MF}}>0.4$.

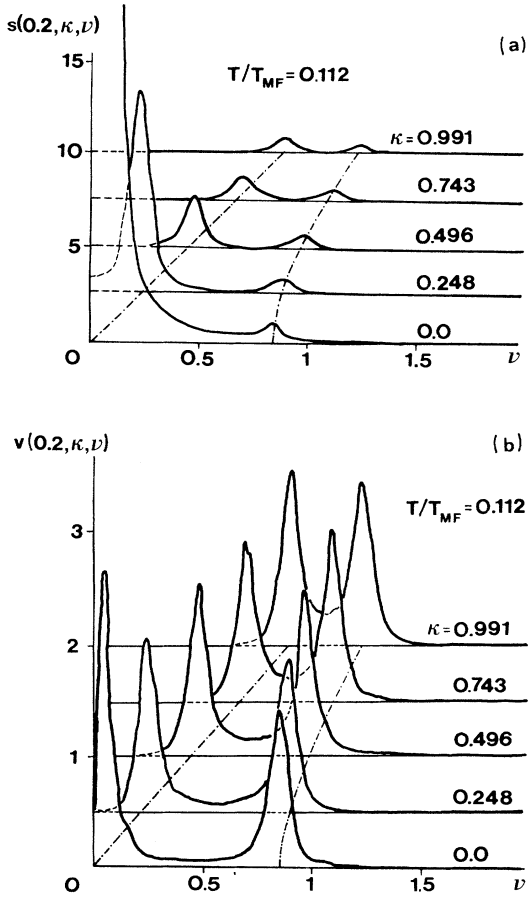

FIG. 3. (a) Dynamic structure factor as a function of dimensionless frequency and the wave vector for $T=0.112T_{\mathrm{MF}}$ ($\vartheta=0.2$). (b) Velocity-velocity correlation function.

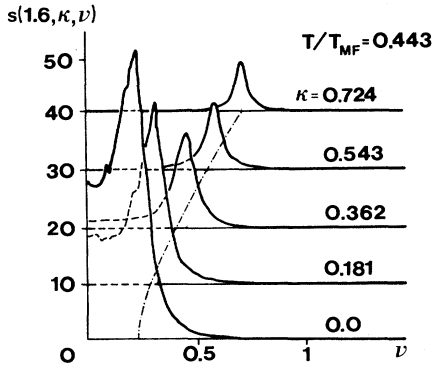

FIG. 4. Same as Fig. 3(a) for $T/T_{\rm MF}=0.443$ ($\vartheta=1.6$).

the $k=0$ phonon becomes overdamped. Figure 4 shows the situation just above this point ($\vartheta=1.6$, $T/T_{\rm MF}=0.44$). The situation with the overdamped $k=0$ phonon persists down to $0.3T_{\rm MF}$ ($\vartheta\approx 0.8$).

Below $\vartheta=0.6$ the behavior of $s(\vartheta,0,\nu)$ is shown in Fig. 1. In this region the damping starts to diminish, and the phason and amplitudon peak appear. The phason peak is dominant in $S(k,\omega)$. However, the phase and amplitude modes contribute equally to the well-known sum rule

$$\int_0^\infty (d\omega/2\pi)V(k,\omega)=T/2m\ ,$$
$$\int_0^\infty (d\nu/2\pi)v(\vartheta,\kappa,\nu)=(T/2m)[b/\Omega^3(mc)^{1/2}]\ , \qquad (12)$$

for the velocity-velocity correlation function

$$V(k,\omega)=\text{Fourier transform of } \langle \dot{\psi}_1(x,t)\dot{\psi}_1(0,0)\rangle$$
$$=\omega^2 S(k,\omega)\ , \qquad (13)$$

and for its dimensionless counterpart

$$v(\vartheta,k/K,\omega/\Omega)=[b/\Omega^2(mc)^{1/2}]V(k,\omega)$$
$$=(\omega/\Omega)^2 s(\vartheta,k/K,\omega/\Omega)\ . \qquad (14)$$

This situation is illustrated in Fig. 1(b) for a range of ϑ's at $\kappa=0$ and in Fig. 3(b) for a range of κ's at $\vartheta=0.20$. The

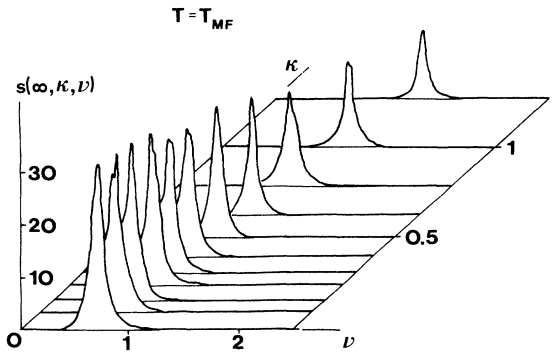

FIG. 5. Dynamic structure factor as a function of reduced variables at $T=T_{\rm MF}$ (quartic case, $\vartheta=\infty$).

widths of the phason and amplitudon peaks in $S(k,\omega)$ are equal and linear in temperature. The reason for that follows from the picture in which the dynamics of phase and amplitude fluctuations are separated.[4] Even when both of them are harmonic and free of damping, the phase fluctuations enter into $S(k,\omega)$ through $\exp(i\chi)$ and thus convolute with amplitude fluctuations.

The comparison with experiment in the temperature region $T\ll T_{\rm MF}$ is not straightforward. The phase and amplitude separation can be seen in the experiment as well as the equipartition of the oscillator strength between these modes. The temperature dependence of $S(k,\omega)$ in the real system is modified below T_x by 3D couplings which generally cause faster transformation toward the Peierls phase. Below T_p the Bragg elastic peak appears at the Peierls wave vector instead of the diffuse spot. In blue bronze[2,10] $T_p=182$ K is considerably higher than $0.3T_{\rm MF}$, and strictly one-dimensional phase-amplitude separation may not actually be seen there. The situation may be better in transition-metal tetrachalcogenides $(MX_4)_nI$, where the ratio $T_{\rm MF}/T_p$ is higher. However, more detailed neutron experiments on these compounds are needed for a comparison.

Considering strictly one-dimensional (incommensurate Peierls) systems, our simulations, combined with previous knowledge, may give a rather complete picture of what is going on in the lattice. We may now ask, what is the implication of our results on the electronic subsystem?

ELECTRONIC PSEUDOGAP

It is well known that lattice fluctuations toward the Peierls state show up in the electronic spectrum as a pseudogap which transforms to the ordinary gap below the three-dimensional Peierls temperature. Above the transition the density of states in the pseudogap influences the optical, electrical, and magnetic properties of the system.[4,9] Different forms for the pseudogap have been predicted in the literature within two basically different approaches. In the first approach,[11] elaborated many years ago, the pseudogap was calculated from the low-order electronic self-energy correction due to coupling to the Kohn-Peierls phonons. The important point in this calculation is that under appropriate conditions[12] only the static structure factor $S(q)$ of the lattice enters in the expression for the self-energy. Combined with a numerical transfer-matrix calculation of the static structure factor,[7] this led to the determination of the electronic density of states in a wide temperature range above and below $T_{\rm MF}$. This approach is valid only provided that the higher-order corrections to the electron self-energy are not important. Later on this was partially improved by calculating the electron self-energy to infinite order in the external random field[13] with the static correlation function given by $S(q)$.

All these calculations[11–13] predict an electronic density of states which slowly decreases toward the center of the pseudogap. A much faster (exponential) decrease of the density of states was found in the second, essentially low-temperature, approach. In this approach, which was thought to apply up to very close to $T_{\rm MF}$, the phase-

amplitude separation was assumed from the outset and the perturbative effect of the phase and amplitude fluctuations on the electrons with an ordinary gap in their spectrum was considered.

Our results for $S(k,\omega)$ allow us to comment on these two results to the pseudogap. While the first approach definitively does not apply at very low temperatures where the second approach is correct, it is also clear that the second approach based on the amplitude-phase separation does not apply above $0.3T_{\mathrm{MF}}$, where the dynamics of the system is described by a single mode. It seems appropriate to use the first approach in this temperature range, especially above $0.4T_{\mathrm{MF}}$.

CONCLUSION

The transformation of the phonon to the amplitude and phase mode on lowering the temperature are studied for the one-dimensional Peierls system. The situation near T_{MF} was quantitatively compared with the experimental findings on blue bronze. For lower temperatures only qualitative comparison is possible because of the increasing importance of interchain couplings. Temperature regions with different shapes of the electronic pseudogap are identified.

ACKNOWLEDGMENTS

Helpful discussions with J. P. Pouget, I. Batistić, and A. Bjeliš are gratefully acknowledged. This work was supported in part by the Yugoslavia-U.S. research project No. DOE PN 738 and research project No. Yu-ECC CI1*0526-M(CD).

[1]R. Comes and G. Shirane, in *Highly Conducting One-Dimensional Solids*, edited by J. T. Diversee, R. P. Evrard, and V. E. van Doren (Plenum, New York, 1979), and references therein.

[2]J. P. Pouget, C. Escribe-Filippini, B. Hennion, R. Currat, A. H. Mouden, R. Moret, J. Marcus, and C. Schlenker, Mol. Cryst. Liq. Cryst. **121**, 111 (1985).

[3]D. Allender, J. W. Bray, and J. Bardeen, Phys. Rev. B **9**, 119 (1974).

[4]S. A. Brazovskii and I. E. Dzyaloshinskii, Zh. Eksp. Teor. Fiz. **71**, 2338 (1976).

[5]E. Tutiš and S. Barišić, Europhys. Lett. **8**, 155 (1989).

[6]D. Beeman, J. Comput. Phys. **20**, 130 (1976).

[7]D. J. Scalapino, M. Sears, and R. A. Ferrell, Phys. Rev. B **6**, 3409 (1972).

[8]E. Bonam, J. Stat. Phys. **39**, 167 (1985).

[9]P. A. Lee, T. M. Rice, and P. W. Anderson, Solid State Commun. **14**, 703 (1974).

[10]J. P. Pouget, B. Hennion, C. Escribe-Filippini, and M. Sato, preceding paper, Phys. Rev. B **43**, 8421 (1991); J. P. Pouget, S. Girault, A. H. Moudden, B. Hennion, C. Escribe-Filippini, and M. Sato, Phys. Scr. T **25**, 58 (1989).

[11]P. A. Lee, T. M. Rice, and P. W. Anderson, Phys. Rev. Lett. **31**, 462 (1973).

[12]A. Bjeliš and S. Barišić, J. Phys. (Paris) Lett. **36**, L169 (1975).

[13]M. V. Sadovskii, Zh. Eksp. Theor. Fiz. **77**, 2070 (1979).